

## GaN/AlGaIn heterojunction infrared detector responding in 8–14 and 20–70 $\mu\text{m}$ ranges

G. Ariyawansa, M. B. M. Rinzan, M. Strassburg, N. Dietz, and A. G. U. Perera<sup>a)</sup>  
*Department of Physics and Astronomy, Georgia State University, Atlanta, Georgia 30303*

S. G. Matsik  
*NDP Optronics LLC, Mableton, Georgia 30126*

A. Asghar and I. T. Ferguson  
*School of Electrical and Computer Engineering, Georgia Institute of Technology, Atlanta, Georgia 30332*

H. Luo and H. C. Liu  
*Institute for Microstructural Sciences, National Research Council, Ottawa K1A 0R6, Canada*

(Received 19 April 2006; accepted 21 August 2006; published online 5 October 2006)

A GaN/AlGaIn heterojunction interfacial work function internal photoemission infrared detector responding in 8–14 and 20–70  $\mu\text{m}$  ranges has been demonstrated. Free carrier absorption based photoresponse shows a wavelength threshold of 14  $\mu\text{m}$  with a peak responsivity of 0.6 mA/W at 80 K under  $-0.5$  V bias. A sharp peak in the 11–13.6  $\mu\text{m}$  range is observed superimposed on the free carrier response. In addition, the work demonstrates 54  $\mu\text{m}$  (5.5 THz) operation of the detector based on  $1s-2p\pm$  transition of Si donors in GaN. Possible approaches on improving the performance of the detector are also addressed. © 2006 American Institute of Physics. [DOI: 10.1063/1.2360205]

The well studied GaAs/AlGaAs material system has been the material of interest for developing infrared (IR) devices during the past few decades. GaAs/AlGaAs detectors covering a wide range from near infrared (NIR) to FIR<sup>1–4</sup> have been developed using different concepts and techniques. Due to the rapid development of group III-As based device structures, mainly detectors, lasers,<sup>5</sup> and focal plane arrays,<sup>6</sup> optimization of devices has been readily achieved. Further improvements may require the use of other material systems, which have advantages in different regions compared to the GaAs/AlGaAs system. For example, the reststrahlen region of GaAs can be accessible with other material systems. Currently, as a group III-V material, GaN has attracted the attention of the scientific community in developing electronic and optoelectronic devices. GaN/AlGaIn device structures, such as ultraviolet (UV) light emitting diodes,<sup>7</sup> multiple quantum well light emitting devices,<sup>8,9</sup> Schottky photodetectors,<sup>10</sup> and heterojunction photodetectors,<sup>11</sup> have been already demonstrated. Using the GaN/AlGaIn system, mid-infrared (Ref. 12) and MIR (Ref. 13) quantum well infrared photodetectors have been demonstrated. Also photodiodes operating in the UV region are available for a wide variety of commercial applications. However, detectors working in the long wave or very long wave IR regions based on group III-nitrides are still in the initial development stage. At present, the growth of high-quality GaN/AlGaIn heterostructures is limited by the availability of suitable lattice-matched substrate materials and process/material knowledge base, which has to be overcome for more advanced optoelectronic device structures.

In this letter, the operation of a GaN/AlGaIn heterojunction interfacial work function internal photoemission (HEIWIP) IR detector<sup>14</sup> responding in the 8–14 and

20–70  $\mu\text{m}$  ranges is demonstrated. The wide band gap of GaN reduces interband tunneling relative to GaAs, and the higher effective mass would reduce the thermal emission, leading to better performance.

The HEIWIP structure was grown by metal-organic chemical-vapor deposition on a sapphire substrate. As schematically shown in Fig. 1(a), the GaN/AlGaIn HEIWIP structure consists of a  $n^+$ -doped GaN emitter layer (which also serves as the top contact), an undoped  $\text{Al}_x\text{Ga}_{1-x}\text{N}$  barrier layer with  $x$  of 0.026, and a  $n^+$ -doped GaN bottom contact

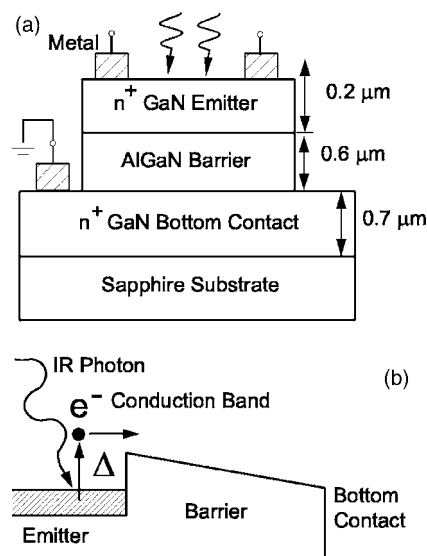


FIG. 1. (a) Schematic diagram of the GaN/AlGaIn HEIWIP structure. The doping concentration of the GaN emitter is  $5 \times 10^{18} \text{ cm}^{-3}$ , while the GaN bottom contact is doped to  $5 \times 10^{18} \text{ cm}^{-3}$ . The AlGaIn barrier is not intentionally doped. By design, the Al fraction of AlGaIn is set to 0.026 in order to have 14  $\mu\text{m}$  wavelength threshold. (b) The band diagram showing the conduction band profile. The band offset  $\Delta$  determines the wavelength threshold.

<sup>a)</sup>Electronic mail: uperera@gsu.edu

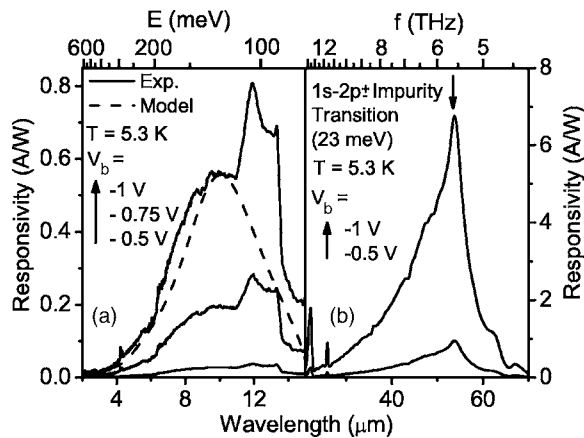


FIG. 2. (a) Spectral response of the detector measured at 5.3 K under different biases and the calculated free carrier response fitted with the experimental curve at  $-1$  V. The sharp drop at  $14 \mu\text{m}$  is due to the reststrahlen in GaN. The broad peak in the  $11\text{--}13.6 \mu\text{m}$  region on the free carrier response is probably due to carbon impurities and/or nitrogen vacancies in the structure. (b) Response at  $54 \mu\text{m}$  ( $5.5$  THz) based on  $1s\text{--}2p\pm$  transition of Si donors in GaN.

layer. Si was used as the  $n$ -type dopant. The structure was processed to form square mesa elements of different areas by dry etching techniques. The Ohmic contacts were formed by deposition of Ti/Al/Ti/Au (metalization) on the top and bottom contact layers. After the metalization, the device structure was annealed under a  $\text{N}_2$  gas flow at  $700^\circ\text{C}$  temperature for 2 min. The annealed sample was mounted on a chip carrier and wire bonds were made from each mesas of the sample to the chip carrier. Current-voltage ( $IV$ ) measurements were performed, by using a Keithley 2400 source meter, on all the mesas of the sample in order to check for uniformity of the structure. Spectral measurements for normal incidence radiation were carried out on several uniform mesas, by using a Perkin Elmer System 2000 Fourier transform infrared (FTIR) spectrometer. The spectra were calibrated relative to a background spectra obtained by a Si composite bolometer with the same set of optical components.

The band diagram indicating the conduction band profile and the transition of electrons leading to free carrier response is shown in Fig. 1(b). The detection mechanism<sup>14</sup> involves free carrier absorption in the emitter, followed by internal photoemission of photoexcited carriers across the interfacial barrier, and then collection of carriers by the applied electric field at the contacts. The offset between the Fermi level in the emitter layer and the conduction band edge of the barrier layer forms the interfacial work function ( $\Delta$ ), which arises due to band offset of different materials and band gap narrowing<sup>15</sup> of the highly doped emitter layer. The threshold wavelength  $\lambda_0$  (in micrometers) is given by  $1240/\Delta$ , where  $\Delta$  is in meV.

The variation of the detector response in the  $8\text{--}14 \mu\text{m}$  range with bias at 5.3 K is shown in Fig. 2(a). The calculated response at  $-1$  V bias is also shown in the figure. The detector has a  $14 \mu\text{m}$  zero response threshold ( $\lambda_0$ ) with a peak at  $12 \mu\text{m}$ . The reststrahlen absorption of GaN falls in the  $14\text{--}20 \mu\text{m}$  region, drastically reducing the photoresponse, as evident from the figure. The spectral measurements performed on several mesas confirm that the detector response is consistent. The response in the  $8\text{--}14 \mu\text{m}$  region is due to free carrier absorption, as expected from the theoretical calculation. The calculation is based on a model<sup>14</sup> in which the

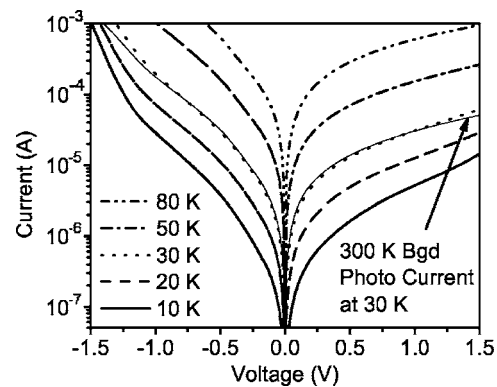


FIG. 3. Current-voltage curves at different temperatures under dark condition and the 300 K background photocurrent at 30 K. The detector has a BLIP of 30 K, and this is lower than the expected BLIP temperature due to the response at  $54 \mu\text{m}$ .

complex permittivity is calculated by the Lorentz-Drude theory, and the light propagation in the structure is derived from the transfer matrix method. The responsivity  $R$  is given by  $R = \eta g_p q \lambda / hc$ , where  $\eta$  is the total quantum efficiency,  $g_p$  is the photoconductive gain,  $q$  is the electron charge,  $\lambda$  is the wavelength,  $h$  is the Planck constant, and  $c$  is the speed of light. The detector has a peak responsivity of  $0.8$  A/W and a detectivity of  $2.5 \times 10^{10}$  Jones at 5.3 K. The responsivity drastically decreases with decreasing bias, and zero response was observed at 0 V bias, confirming no photovoltaic effect exists. A similar but slightly weaker response was observed for the detector under forward bias. The photoconductive gains at  $-1$ ,  $-0.75$ , and  $-0.5$  V biases are 1.3, 0.7, and 0.4, respectively.

The broad peak superimposed on the free carrier response in the  $11\text{--}13.6 \mu\text{m}$  region might be due to carbon impurities or nitrogen vacancies. The reported donor ionization energy of carbon<sup>16</sup> falls in the  $0.11\text{--}0.14$  eV range, while the binding energy of N vacancy<sup>17</sup> is about 0.1 eV. As the donors in the barrier will be widely scattered, they will act as a hydrogenic atom, and the standard hydrogenic energy level model can be used to determine the location of absorption peaks associated with a given transition. Carbon can be unintentionally introduced into GaN during the growth, either as a donor at a Ga site or as an acceptor at a N site, mainly through the organic precursors. Assuming that the two peaks observed at  $11.9 \mu\text{m}$  ( $104.2$  meV) and  $13.3 \mu\text{m}$  ( $93.2$  meV) are due to transitions to the first impurity excited state, the ionization energies were calculated to be 139 and 124 meV, respectively. These ionization energy values in the  $140\text{--}110$  meV range support the assumption that the corresponding transitions are carbon donor related impurity transitions. Transitions related to carbon acceptors ( $0.89$  eV of ionization energy)<sup>16</sup> fall out of the spectral range reported here (below  $1.4 \mu\text{m}$ ), although the carbon acceptors are preferred in GaN.<sup>18</sup> The measurements performed on different devices provide consistent results. For detectors with a threshold above  $14 \mu\text{m}$ , these impurity transitions enhance the response. Detectors designed to have shorter thresholds (below  $14 \mu\text{m}$ ) operating at high temperatures will not show the expected performance at the designed temperature, because the thermal excitations take place through impurity states. However, to reduce the incorporation of carbon, which affects the IR detector response, alternative group III precursors can be explored.

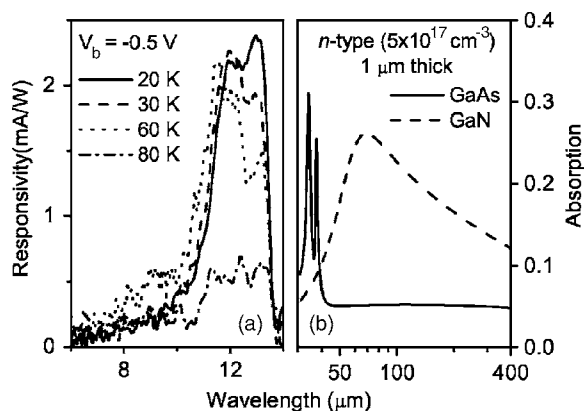


FIG. 4. (a) Spectral response measured at 20, 30, 60, and 80 K under  $-0.5$  V bias. The  $10$ – $14$   $\mu\text{m}$  response decreased in strength as the temperature increased beyond 60 K. (b) Comparison of calculated IR absorption by  $1$   $\mu\text{m}$  thick GaAs and GaN films.

As shown in Fig. 2(b), a sharp peak at  $54$   $\mu\text{m}$  ( $5.5$  THz) is also observed. The corresponding energy for the transition leading to this peak is  $23$  meV. Researchers<sup>19</sup> have found the donor binding energy of Si in GaN to be  $29$  meV, and the transition from  $1s$  to  $2p_{\pm}$  level occurs at  $21.9$  meV. Moore *et al.*<sup>20</sup> has reported the  $1s$ – $2p_{\pm}$  transition of Si in GaN at  $23.3$  meV and donor effective mass binding energy of  $31.1$  meV. Hence, the sharp response peak observed at  $23$  meV can be identified as  $1s$ – $2p_{\pm}$  transition of Si donors in GaN. Infrared absorption measurement is a well known technique to identify the shallow impurities such as Si in GaN. This study not only confirms the  $1s$ – $2p_{\pm}$  transition of Si in GaN but also results in a GaN/AlGaIn terahertz detector. Since the donor states of Si in intentionally doped GaN are quite understood and stable, a  $5.5$  THz detector could be developed based on  $1s$ – $2p_{\pm}$  transition, and a promising result is reported for an unoptimized detector.

The dark current-voltage ( $I$  $V$ ) characteristics of the detector at different temperatures, along with the  $300$  K background photocurrent curve measured at  $30$  K, are shown in Fig. 3. Based on the dark and the photocurrent measurements, the background limited infrared performance (BLIP) temperature is obtained to be  $30$  K. The BLIP temperature may have been reduced due to the terahertz response which is visible at low temperature. The response below  $14$   $\mu\text{m}$  can be obtained up to  $80$  K, and Fig. 4(a) shows the responsivity at  $20$ ,  $30$ ,  $60$ , and  $80$  K under  $-0.5$  V bias. The response at  $80$  K is weak, only showing the signature of the response in the  $10$ – $14$   $\mu\text{m}$  region.

A comparison between the absorption of FIR radiation by a  $1$   $\mu\text{m}$  thick GaAs film and a GaN film is shown in Fig. 4(b). Both films are  $n$  doped to a density of  $5 \times 10^{17}$   $\text{cm}^{-3}$ . Due to higher absorption in the region above  $40$   $\mu\text{m}$ , GaN would be a good candidate for FIR detector development. The GaN/AlGaIn detector reported in this letter is not optimized to have the best performance in the  $8$ – $14$   $\mu\text{m}$  range. The response of the current single period detector can be significantly enhanced by incorporating multiperiods of emitter/barrier layers. In comparison with a GaAs/AlGaAs HEIWIP detector<sup>21</sup> with multiperiods responding in the  $5$ – $20$   $\mu\text{m}$  range, the reported GaN/AlGaIn detector has a higher response even with a single period. However, the detectivity is lower than the GaAs/AlGaAs detector. This could

be due to the increased dark current (also the increased noise current) as a result of the response at  $54$   $\mu\text{m}$  due to the transitions of Si impurity atoms in GaN. Moreover, resonant cavity enhancement<sup>14</sup> could be used to increase the performance of the detector further.

In summary, a GaN/AlGaIn HEIWIP detector responding in the  $8$ – $14$  and  $20$ – $70$   $\mu\text{m}$  regions is reported. The response in the  $8$ – $14$   $\mu\text{m}$  range is due to free carrier absorption in the structure, while the response at  $54$   $\mu\text{m}$  ( $5.5$  THz) is based on  $1s$ – $2p_{\pm}$  transition of Si donors in GaN. Some minor response contributions associated with impurity states in the system were also observed. The promising initial results demonstrate the possibility of GaN/AlGaIn IR detectors with improved performance compared to GaAs/AlGaAs based detectors.

This work is supported in part by the U.S. Air Force Small Business Innovation Research Program (SBIR) under Grant No. FA9453-05-M-0106. The authors would like to acknowledge Dave Cardimona and Tzveta Apostolova for fruitful discussions and the support and Rongzhu Wang and Hun Kang for technical assistance.

<sup>1</sup>M. P. Touse, G. Karunasiri, K. R. Lantz, H. Li, and T. Mei, Appl. Phys. Lett. **86**, 093501 (2005).

<sup>2</sup>J. Li, K. K. Choi, and D. C. Tsui, Appl. Phys. Lett. **86**, 211114 (2005).

<sup>3</sup>H. Luo, H. C. Liu, C. Y. Song, and Z. R. Wasilewski, Appl. Phys. Lett. **86**, 231103 (2005).

<sup>4</sup>M. B. M. Rinzan, A. G. U. Perera, S. G. Matsik, H. C. Liu, Z. R. Wasilewski, and M. Buchanan, Appl. Phys. Lett. **86**, 071112 (2005).

<sup>5</sup>Z. Mi, P. Bhattacharya, and S. Fathpour, Appl. Phys. Lett. **86**, 153109 (2005).

<sup>6</sup>Sanjay Krishna, Darren Forman, Senthil Annamalai, Philip Dowd, Petros Varangis, Tom Tumolillo, Jr., Allen Gray, John Zilko, Kathy Sun, Mingguo Liu, Joe Campbell, and Daniel Carothers, Appl. Phys. Lett. **86**, 193501 (2005).

<sup>7</sup>J. P. Zhang, X. Hu, Yu. Bilenko, J. Deng, A. Lunev, M. S. Shur, R. Gaska, M. Shatalov, J. W. Yang, and M. A. Khan, Appl. Phys. Lett. **85**, 5532 (2004).

<sup>8</sup>W. H. Sun, J. W. Yang, C. Q. Chen, J. P. Zhang, M. E. Gaeviski, E. Kuokstis, V. Adivarahan, H. M. Wang, Z. Gong, M. Su, and M. Asif Khan, Appl. Phys. Lett. **83**, 2599 (2003).

<sup>9</sup>Madalina Furis, A. N. Cartwright, Hong Wu, and William J. Schaff, Appl. Phys. Lett. **83**, 3486 (2003).

<sup>10</sup>M. Asif Khan, J. N. Kuznia, D. T. Olson, M. Blasingame, and A. R. Bhattarai, Appl. Phys. Lett. **63**, 2455 (1993).

<sup>11</sup>S. K. Zhang, W. B. Wang, I. Shtau, F. Yun, L. He, H. Morko, X. Zhou, M. Tamargo, and R. R. Alfano, Appl. Phys. Lett. **81**, 4862 (2002).

<sup>12</sup>Daniel Hofstetter, Sven-Silvius Schad, Hong Wu, William J. Schaff, and Lester F. Eastman, Appl. Phys. Lett. **83**, 572 (2003).

<sup>13</sup>Claire Gmachl, Hock M. Ng, and Alfred Y. Cho, Appl. Phys. Lett. **77**, 334 (2000).

<sup>14</sup>D. G. Esaev, M. B. M. Rinzan, S. G. Matsik, and A. G. U. Perera, J. Appl. Phys. **96**, 4588 (2004).

<sup>15</sup>W. Z. Shen, A. G. U. Perera, H. C. Liu, M. Buchanan, and W. J. Schaff, Appl. Phys. Lett. **71**, 2677 (1997).

<sup>16</sup>V. Bougrov, M. Levinshtein, S. Rumyantsev, and A. Zubrilov, in *Gallium Nitride (GaN)*, edited by M. E. Levinshtein, S. L. Rumyantsev, and M. S. Shur (Wiley, NY, 2001), p. 1.

<sup>17</sup>M. Sumiya, K. Yoshimura, K. Ohtsuka, and S. Fuke, Appl. Phys. Lett. **76**, 2098 (2000).

<sup>18</sup>P. Bogusławski, E. L. Briggs, and J. Bernholc, Appl. Phys. Lett. **69**, 233 (1996).

<sup>19</sup>Y. J. Wang, R. Kaplan, H. K. Ng, K. Doverspike, D. K. Gaskill, T. Ikeda, I. Akasaki, and H. Amano, J. Appl. Phys. **79**, 8007 (1996).

<sup>20</sup>W. J. Moore, J. A. Freitas, Jr., and R. J. Molnar, Phys. Rev. B **56**, 12073 (1997).

<sup>21</sup>S. G. Matsik, M. B. M. Rinzan, D. G. Esaev, A. G. U. Perera, H. C. Liu, and M. Buchanan, Appl. Phys. Lett. **84**, 3435 (2004).